optica

Photorealistic full-color nanopainting enabled by a low-loss metasurface

Pengcheng Huo,[1,2,†] Maowen Song,[1,2,†] Wenqi Zhu,[3,4,†] Cheng Zhang,[5,†] Lu Chen,[3,4] Henri J. Lezec,[3] Yanqing Lu,[1,2,6] Amit Agrawal,[3,4] and Ting Xu[1,2,7]

[1]National Laboratory of Solid-State Microstructures, College of Engineering and Applied Sciences, Nanjing University, Nanjing 210093, China
[2]Collaborative Innovation Center of Advanced Microstructures, Nanjing 210093, China
[3]Physical Measurement Laboratory, National Institute of Standards and Technology, Gaithersburg, Maryland 20877, USA
[4]Maryland NanoCenter, University of Maryland, College Park, Maryland 20742, USA
[5]School of Optical and Electronic Information and Wuhan National Laboratory for Optoelectronics, Huazhong University of Science and Technology, Wuhan 430074, China
[6]e-mail: yqlu@nju.edu.cn
[7]e-mail: xuting@nju.edu.cn

Received 21 July 2020; accepted 29 July 2020 (Doc. ID 403092); published 4 September 2020

We realize a dielectric metasurface that enables full-color generation and ultrasmooth brightness variation. The reproduced artwork "girl with a pearl earring" features photorealistic color representation and stereoscopic image impression, mimicking the texture of an oil-painting.

https://doi.org/10.1364/OPTICA.403092

Color, originating from light-matter interactions, is one of the primary attributes of human visual perception and carries information critical for imaging and display technology. In recent years, enabled by remarkable developments in nanofabrication technology, the research field of subwavelength structural coloring has seen extensive growth [1–10]. For example, optical metasurfaces, composed of an array of deep-subwavelength nanostructures, offer opportunities to tailor the spectrum of incoming light and generate vivid structural colors by simply varying the nanostructure dimensions. Preliminary research in this area utilized localized plasmon resonances supported by metallic nanostructures to achieve structural colors because of their strong dependence on the geometry of nanostructures [1–8]. More recently, metasurfaces based on dielectric nanostructures have also demonstrated the ability to produce vibrant colors, realized by leveraging the electric and magnetic Mie resonances supported by individual dielectric nanostructures [9,10]. Usually, structural color engineering using metasurfaces is targeted to obtain high color gamut and saturation, and thus it is expected that the amplitude of incident light for a desired color (wavelength) is well preserved upon transmission or reflection through the metasurface. As a result, though such metasurfaces exhibit high transmission or reflection efficiency, the brightness of the generated color is fixed. Note that, in addition to color gamut and saturation, brightness is also one of the fundamental properties of color and represents the chiaroscuro of an image. By tuning the brightness of a color, the generated shadow rendering effect can make an image appear with a stronger space and stereo perception. Although metasurfaces incorporated with liquid crystals [11] and electrochromic polymers [12] can control the amplitude of generated colors, complicated electrical device architectures and incomplete full-color spectral response significantly hinders their practical use. Hence, the ability to efficiently and smoothly control the brightness of structural color across the entire visible spectral range is an important functionality required for various applications including high precision nanopainting.

Here, we design and experimentally demonstrate a low-loss dielectric metasurface-enabled brightness-tunable full-color nanopainting, and reproduce the famous artwork "girl with a pearl earring" [13], mimicking the vivid visual impact and texture of an oil-painting. The metasurface consists of a periodic arrangement of titanium dioxide (TiO_2) nanopillars with spatially varying dimension and orientation, which, respectively, determine the hue and brightness of the output colors. This feature is highly beneficial because it allows multiple degrees of freedom to upgrade the impression of a full-color nanopainting, as we demonstrate below.

Figure 1(a) presents the schematic of the metasurface consisting of TiO_2 nanopillars supported on a silicon dioxide (SiO_2) substrate. TiO_2 is chosen as constituent material due to its low-loss and high refractive-index in the visible spectral range. Each nanopillar constituting the metasurface is designed to act as a narrowband halfwaveplate capable of efficiently rotating the polarization of normally incident linearly polarized light only at specific design wavelengths. For example, a nanopillar with its long-axis oriented at 45° relative to the incident electric-field converts y-polarized incident light to its cross-polarized state at the design wavelength, whereas the unrotated light at other wavelengths are blocked by an analyzer placed after the metasurface. Based on Malus's law [14], the output intensity (I) transmitted through a polarizer-analyzer combination at the design wavelength is determined by the relative angle between the polarization axis of the polarizer and the electric field orientation of the transmitted light, where the latter can be readily modulated by spatially varying the orientation angle (θ) of individual nanopillars. Therefore, the metasurface nanopillar

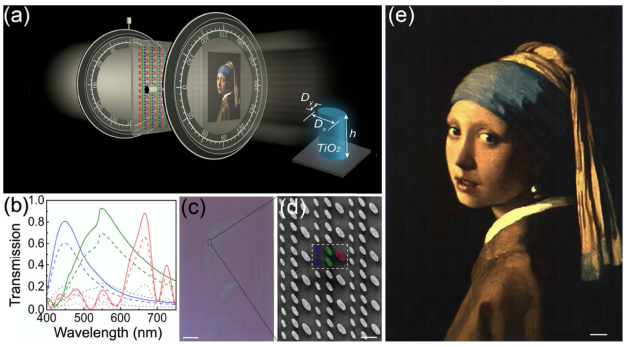

Fig. 1. (a) Schematics of the full-color nanopainting generation setup. The inset shows a single TiO_2 nanopillar supported by an SiO_2 substrate. (b) The calculated cross-polarization conversion transmission for the B (blue curves), G (green curves), and R (red curves) colors when the orientation angle θ of the nanopillar is varied from 45° (solid lines) to 30° (dashed lines) and 15° (dotted lines). (c) Optical image of the fabricated pattern in reflection mode without any polarizers. Scale bar represents 100 μm. (d) Scanning electron micrograph (SEM) of the highlighted area in (c), a super-cell is enclosed by white dashed lines and the false coloring of the nanopillars indicate the primary colors that are generated by the respective nanopillars. Scale bar represents 500 nm. (e) Experimental color printing of "girl with a pearl earring". Scale bar represents 50 μm.

dimensions are spatially altered to generate a desired structural color, and their orientation is varied to tune the brightness as $I = I_0 \sin^2(2\theta)$, where I_0 is the input intensity. Here, corresponding to the target filtering colors blue (B), green (G), and red (R), we design a set of elliptical nanopillars with the lengths of major and minor axis (D_x, D_y) of (250 nm, 50 nm), (320 nm, 80 nm), and (440 nm, 170 nm), respectively. The height of all the nanopillars is fixed at 600 nm. In order to create arbitrary color patterns by uniting nanopillars in a geometrically nonconflicting manner, the dimensions of unit-cell for blue, green, and red wavelengths are optimized as 370 nm × 370 nm, 370 nm × 370 nm, and 370 nm × 740 nm, respectively. The calculated transmission magnitudes of cross-polarization for B, G, and R pixels for three different θ angles are depicted in Fig. 1(b). As expected, a single prominent peak can be observed for each spectrum, located at approximately 450 nm, 540 nm, and 660 nm, corresponding respectively to blue, green, and red colors. With changing θ, the profile of the spectra smoothly varies, indicating different color brightness.

By encoding the brightness and color information into the spatially varying nanopillars, the nanoprinted image enables photorealistic color presentation and stereoscopic impression. As a proof of concept, the famous artwork "girl with a pearl earring" is selected as a target image for printing with the above-designed RGB unit-cells. For fabrication, electron beam lithography together with atomic layer deposition of TiO_2 and dry etching, as described in Ref. [15], are employed to realize the metasurface patterns. Figures 1(c) and 1(d) show the overview optical image without any polarizers and enlarged SEM image of the area enclosed by black lines to illustrate the detailed arrangement of the nanopillars. The high-resolution image generated by the full color metasurface upon white-light illumination under orthogonal polarizer-analyzer orientation is presented in Fig. 1(e). It can be observed that the girl wears a blue turban and a gold jacket with a white-collar underneath which presents ultra-smooth brightness transitions, and the darker peripheral sides blend seamlessly with the black background. The smooth color hue and brightness transitions allow the image to present an oil painting-like texture, elegantly bridging the gap between scientific results and art.

In conclusion, our judiciously designed TiO_2 metasurface exhibits a full-color gamut and customized color brightness profile. The spatially varying nanopillars provide extraordinary capabilities for high-resolution nanopainting and seamless mixing of colors. We envision such a color and brightness tuning metasurface to provide a promising platform for applications in both the sciences and the arts.

Funding. Ministry of Science and Technology of the People's Republic of China (2017YFA0303700); National Natural Science Foundation of China (11774163); University of Maryland (70-NANB14H209).

Acknowledgment. W. Z., L. C., and A. A. acknowledge support under the Cooperative Research Agreement between the University of Maryland and the NIST through the University of Maryland. Feedback from Motoko Lezec of the Smithsonian is gratefully acknowledged.

Disclosures. The authors declare no conflicts of interest.

†These authors contributed equally to this Letter.

REFERENCES

1. T. Xu, Y. K. Wu, X. Luo, and L. J. Guo, Nat. Commun. **1**, 59 (2010).
2. K. Kumar, H. Duan, R. S. Hegde, S. C. W. Koh, J. N. Wei, and J. K. W. Yang, Nat. Nanotechnol. **7**, 557 (2012).
3. A. S. Roberts, A. Pors, O. Albrektsen, and S. I. Bozhevolnyi, Nano Lett. **14**, 783 (2014).
4. H. Wang, X. Wang, C. Yan, H. Zhao, J. Zhang, C. Santschi, and O. J. F. Martin, ACS Nano **11**, 4419 (2017).
5. M. Song, X. Li, M. Pu, Y. Guo, K. Liu, H. Yu, X. Ma, and X. Luo, Nanophotonics. **7**, 323 (2018).
6. S. D. Rezaei, R. J. Hong Ng, Z. Dong, J. Ho, E. H. H. Koay, S. Ramakrishna, and J. K. W. Yang, ACS Nano **13**, 3580 (2019).
7. J. Xue, Z. Zhou, L. Lin, C. Guo, S. Sun, D. Lei, C. Qiu, and X. Wang, Light Sci. Appl. **8**, 101 (2019).
8. C. U. Hail, G. Schnoering, M. Damak, D. Poulikakos, and H. Eghlidi, ACS Nano **14**, 1783 (2020).
9. B. Yang, W. Liu, Z. Li, H. Cheng, D.-Y. Choi, S. Chen, and J. Tian, Nano Lett. **19**, 4221 (2019).
10. W. Yang, S. Xiao, Q. Song, Y. Liu, Y. Wu, S. Wang, J. Yu, J. Han, and D.-P. Tsai, Nat. Commun. **11**, 1864 (2020).
11. J. Olson, A. Manjavacas, T. Basu, D. Huang, A. E. Schlather, B. Zheng, N. J. Halas, P. Nordlander, and S. Link, ACS. Nano **10**, 1108 (2016).
12. T. Xu, E. C. Walter, A. Agrawal, C. Bohn, J. Velmurugan, W. Zhu, H. J. Lezec, and A. A. Talin, Nat. Commun. **7**, 10479 (2016).
13. J. Vermeer, Girl with a Pearl Earring, c. 1665.
14. X. Zang, F. Dong, F. Yue, C. Zhang, L. Xu, Z. Song, M. Chen, P. Chen, G. S. Buller, Y. Zhu, S. Zhuang, W. Chu, S. Zhang, and X. Chen, Adv. Mater. **30**, 1707499 (2018).
15. P. Huo, C. Zhang, W. Zhu, M. Liu, S. Zhang, S. Zhang, L. Chen, H. J. Lezec, A. Agrawal, Y. Lu, and T. Xu, Nano Lett. **20**, 2791 (2020).